

2017-07-01

Transfer of ice algae carbon to ice-associated amphipods in the high-Arctic pack ice environment

Brown, Thomas

<http://hdl.handle.net/10026.1/9862>

10.1093/plankt/fbx030

Journal of Plankton Research

Oxford University Press (OUP)

All content in PEARL is protected by copyright law. Author manuscripts are made available in accordance with publisher policies. Please cite only the published version using the details provided on the item record or document. In the absence of an open licence (e.g. Creative Commons), permissions for further reuse of content should be sought from the publisher or author.

1 **Transfer of ice algae carbon to ice-associated amphipods**
2 **in the high-Arctic pack ice environment**

3
4 **Thomas A. Brown^{1,2*}, Philipp Assmy³, Haakon Hop^{3,4}, Anette Wold³ and Simon T. Belt²**

5 ¹ Marine Ecology and Chemistry, Scottish Association for Marine Science, Oban, Argyll,
6 UK, PA37 1QA.

7 ² School of Geography, Earth and Environmental Sciences, University of Plymouth,
8 Plymouth PL4 8AA, UK

9 ³ Norwegian Polar Institute, Fram Centre, N-9296 Tromsø, Norway

10 ⁴ Department of Arctic and Marine Biology, Faculty of Biosciences, Fisheries and
11 Economics, UiT The Arctic University of Norway, N-9037 Tromsø, Norway

12 * Corresponding author: Thomas.Brown@sams.ac.uk

13

14

15 ABSTRACT

16 Sympagic (ice-associated) amphipods channel carbon into the marine ecosystem. With Arctic
17 sea ice extent in decline, it is becoming increasingly important to quantify this transfer of
18 sympagic energy. Recently, a method for quantifying sympagic particulate organic carbon
19 (iPOC) in filtered water samples was proposed based on the abundances of the Arctic sea ice
20 biomarker IP₂₅. Here, we tested the hypothesis that adoption of this method could also
21 provide quantitative estimates of iPOC transfer within Arctic amphipods. We analysed five
22 amphipod species collected north of Svalbard and compared findings to some previous
23 studies. Estimates showed that *Onisimus glacialis* and *Apherusa glacialis* contained the most
24 iPOC, relative to dry mass (23.5 ± 4.5 and 9.8 ± 1.9 mg C g⁻¹, respectively), while *Gammarus*
25 *wilkitzkii* had the highest grazing impact on the available ice algae (0.48 mg C m⁻², for an
26 estimated 24 h), equating to 73% of algal standing stock. Our findings are also broadly
27 consistent with those obtained by applying the H-Print biomarker approach to the same
28 samples. The ability to obtain realistic quantitative estimates of iPOC into sympagic and
29 pelagic fauna will likely have important implications for modelling energy flow in Arctic
30 food webs during future climate scenarios.

31

32

33

34

35

36

37 KEYWORDS: Arctic amphipods, organic carbon, IP₂₅, H-Print, Nansen Basin

38 INTRODUCTION

39 Arctic sea ice provides a unique habitat for ice-associated algae, in particular diatoms
40 (Dieckmann and Hellmer, 2010; Leu *et al.*, 2015), which offer food for a wide range of
41 heterotrophic organisms, with some of the most noticeable being certain crustaceans (Arrigo,
42 2014) such as copepods, decapods, euphausiids and amphipods (Arndt and Swadling, 2006).
43 In Arctic waters, analyses of baited traps and sediment traps have demonstrated that
44 amphipods can dominate biomass in such settings (Nygård *et al.*, 2009; Kraft *et al.*, 2010)
45 and so, in turn, provide an important link between sea ice algae and intermediary, as well as
46 higher trophic level consumers, including fish, seabirds and marine mammals (Lønne and
47 Gabrielsen, 1992; Lønne and Gulliksen, 1989; Dalpadado *et al.*, 2016). With Arctic sea ice
48 extent receding (Serreze *et al.*, 2016), there is a growing need to understand the impact of
49 potential changes in the timing, magnitude and composition of ice algal blooms and the
50 consequences for sympagic, pelagic and benthic grazers (Søreide *et al.*, 2013; Leu *et al.*,
51 2015), since ice-associated amphipods are particularly sensitive to changes in sea ice
52 conditions related to climate change (Kraft *et al.*, 2010; Barber *et al.*, 2015).

53 The direct coupling between sympagic (i.e. sea ice associated) and pelagic
54 communities has been demonstrated recently following the identification of the Arctic sea ice
55 diatom biomarker IP₂₅ (Fig. 1; Belt *et al.*, 2007) in ice-associated zooplankton during
56 springtime (Brown and Belt, 2012a). IP₂₅ is a highly branched isoprenoid (HBI) lipid that
57 serves as a selective tracer of ice-derived organic matter since it is only biosynthesized by
58 certain Arctic sympagic diatoms (Belt *et al.*, 2007; Brown *et al.*, 2014c). Although these
59 particular diatoms are generally the minority species, they are, nonetheless, pan-Arctic in
60 distribution (Brown *et al.*, 2014c). The presence and abundance of IP₂₅ in Arctic sea ice
61 correlate well with spring sea ice diatom biomass (Brown *et al.*, 2011), which has led to the
62 use of this lipid as a qualitative biomarker for sea ice particulate organic carbon (iPOC)

63 (Brown *et al.*, 2016). Consistent with this, IP₂₅ has been identified in sinking iPOC (Belt *et*
64 *al.*, 2008; Brown, 2011; Brown *et al.*, 2016), sediments (Belt and Müller, 2013) and animals
65 (Brown *et al.*, 2014a, 2015; Brown and Belt, 2012b) across the Arctic.

66 In a previous case study investigation, the quantification of IP₂₅ in bulk zooplankton
67 from the Amundsen Gulf (Beaufort Sea) between February and June 2008, demonstrated
68 further that analysis of IP₂₅ represents a potentially useful method for confirming the link
69 between ice algae and heterotrophs (Brown and Belt, 2012a). During the sampling period,
70 increases in the grazing impact of zooplankton were inferred based on higher IP₂₅
71 concentrations within zooplankton, signifying an increase in ice algal grazing. However, a
72 more thorough understanding of the effects of declining sea ice thickness and extent, and
73 therefore sympagic algae, on Arctic animals requires more detailed quantification of
74 sympagic carbon consumption, which, until recently, has not been achievable from IP₂₅
75 concentration data alone. However, a more recent study demonstrated that concentrations of
76 IP₂₅ measured in seawater beneath sea ice during the spring melt can be used to obtain
77 quantitative estimates of sinking iPOC (Brown *et al.*, 2016). In essence, quantitative
78 estimates of iPOC in the water column were obtained by combining respective IP₂₅
79 concentrations with the iPOC/IP₂₅ ratio derived from analysis of the overlying sea ice. Using
80 this approach, Brown *et al.* (2016) showed that iPOC accounted for up to 100% of the total
81 organic carbon available to consumers in the upper water column at the time when sympagic
82 algae were being released from the ice matrix.

83 Combined, the previous identification of IP₂₅ in zooplankton (Brown and Belt, 2012a)
84 and the recent demonstration that iPOC could be quantified in the water column (Brown *et*
85 *al.*, 2016), led us to hypothesise that a similar approach could be used to quantify iPOC in
86 Arctic primary consumers, such as some amphipod species that are known to graze on ice
87 algae. Here, we tested this hypothesis by 1) determining the iPOC/IP₂₅ ratio within ice algal

88 aggregates collected beneath sea ice, north of Svalbard in the Nansen Basin, 2) quantifying
89 IP₂₅ in amphipods sampled from beneath sea ice that were observed feeding on ice algae, and
90 3) combining these findings to quantify iPOC in amphipods. Having established a means of
91 quantifying iPOC in amphipods, our aim was to provide the first quantitative estimates of
92 iPOC consumption for *in-situ* ‘autochthonous’ (permanently inhabiting sea ice) amphipod
93 species; *Gammarus wilkitzkii* Fabricius, 1775, *Apherusa glacialis* Hansen, 1887, *Onisimus*
94 *nansenii* Sars, 1900, *Onisimus glacialis* Sars, 1900 and the ‘allochthonous’ (partly ice-
95 associated) amphipod, *Eusirus holmi* Hansen, 1887. To complement the iPOC/IP₂₅ approach,
96 we also calculated the so-called H-Print (Brown *et al.*, 2014d; Brown and Belt, 2017) for
97 each sample, a method that combines the relative abundances of a variety of diatom-derived
98 HBIs, and has been adopted previously to provide semi-quantitative estimates of the
99 proportion of sympagic versus pelagic carbon in zooplankton (Brown and Belt, 2017) fish,
100 seals and marine mammals (Brown *et al.*, 2017).

101

102 **METHOD**

103 **Site description and sample collections**

104 The area of sample collection was in the Nansen Basin north of Nordaustlandet, Svalbard
105 (Fig. 2). Ice algal aggregates and ice-associated amphipods were collected at an ice-station
106 during the ICE12 expedition in July 2012, where the Norwegian Polar Institute research
107 vessel *Lance* was moored to a large drifting ice floe at starting point 82.5°N, 21°E. The drift
108 was southward towards the outer margins of the marginal ice zone (Fig. 2). The sea ice
109 comprised mainly first-year ice and extended over a region where the water depth was up to
110 2500 m.

111

112 **Sampling of ice algal aggregates**

113 Floating ice algal aggregates were collected with a coarse-meshed sieve through a specially
114 drilled ice hole (3.2 m² in size) at 12 h intervals from 29 July – 1 August 2012 (for more
115 details see Assmy *et al.*, 2013). Upon return to the ship, ice algal aggregates were transferred
116 into 50 mL centrifuge tubes and frozen at -20°C.

117

118 **Sampling of amphipods**

119 Samples of amphipods were collected on 24 separate occasions from 28 July – 1 August
120 2012 below the ice by scuba divers using an electrical suction pump with a 500 µm mesh net
121 (Lønne, 1988). Qualitative sampling of amphipods for IP₂₅ analysis was carried out by
122 sampling as many organisms as possible during 40–60 min of diving. The amphipods were
123 sorted by species and frozen at -80 °C in zip-lock plastic bags.

124 Quantitative amphipod sampling was carried out by scuba divers using 50 × 50 cm
125 standard frames (Hop *et al.*, 2000). Electrical suction pumps were used to collect samples
126 from a set area of flat or ridged sea ice by placing these frames 10 times (one replicate
127 sample) in a direction from the dive hole where ice amphipods occurred and exhaled bubbles
128 were absent. Replicates (5 per flat or ridged sea ice) were taken by a single diver in different
129 directions from the dive hole to avoid repeated sampling of the same under-ice area. The
130 samples were preserved in buffered formaldehyde solution at a final concentration of 4% and
131 were subsequently analysed for species composition, abundance and biomass at the Institute
132 of Oceanology, Sopot, Poland. The total length of amphipods was determined from
133 formaldehyde-preserved organisms blotted on filter paper. Abundance estimates (per m²)
134 were made based on the area covered for each replicate sample (2.5 m²).

135

136 **Total organic carbon**

137 Sub-samples (~50 mg) of freeze-dried algae were decarbonated (10% HCl; 10 mL), washed
138 (3 × 10 mL Milli-Q water) and freeze-dried prior to analysis using a Thermoquest EA1110
139 CHN analyser. L-cystine was used as a calibration standard.

140

141 **Lipid extraction and purification**

142 Extraction of HBI lipids from freeze-dried algae and amphipods was carried out using
143 established techniques (Belt *et al.*, 2012; Brown *et al.*, 2014d). An internal standard (9-
144 octylheptadec-8-ene (9-OHD); 10 µL; 2 µg mL⁻¹) was added to enable the quantification of
145 IP₂₅ (Belt *et al.*, 2012). Samples were covered in methanol (4 mL) and amphipods were
146 mechanically crushed using a glass rod. Samples were then sonicated for 10 min. Milli-Q
147 water (1 mL) and hexane (3×4 mL) were added, and then solutions were vortexed (1 min)
148 and centrifuged (2 min; 2500 revolutions min⁻¹). Supernatant solutions containing lipids were
149 transferred to clean vials with glass pipettes and dried (N₂ stream). Extracts were then re-
150 suspended in hexane (1 mL) and fractionated, providing non-polar lipids (IP₂₅ and other
151 HBIs) using column chromatography (5 mL hexane; SiO₂; 0.5 g).

152

153 **Lipid analysis**

154 Analyses of purified non-polar lipid extracts containing IP₂₅ and other HBIs were carried out
155 using gas chromatography–mass spectrometry (GC–MS) (Belt *et al.*, 2012). Total ion current
156 (TIC) chromatograms were used to determine the retention times and mass spectra of HBIs,
157 and these were compared with those of authentic standards (Belt *et al.* 2012) and published
158 literature (Brown 2011 and references therein) for identification purposes.

159

160 **HBI quantification**

161 For gravimetric quantification of IP₂₅, GC–MS responses were obtained in selective ion
162 monitoring (SIM) mode (*m/z* 350.3) and were normalised using instrumental response factors
163 and the masses of internal standard and sample mass (Belt *et al.*, 2012).

164

165 **iPOC quantification**

166 Based on a previous method for estimating iPOC in seawater (Brown *et al.*, 2016), range and
167 mean estimates of the iPOC content of amphipods (iPOC_{amph}) were obtained by combining
168 amphipod IP₂₅ concentrations with iPOC/IP₂₅ ratios derived from an ice algal aggregate
169 sampled on 29 June 2012 (Eq. 1). iPOC_{amph} concentration estimates were obtained for the
170 five amphipod species sampled.

171

172 (1)

$$173 \quad iPOC_{amph} = IP_{25} \text{ (amphipod)} \times \frac{iPOC_{\text{(aggregate)}}}{IP_{25} \text{ (aggregate)}}$$

174

175

176 **HBI biomarker H-Print**

177 H-Prints (%) were calculated using the abundance of pelagic (III) and sympagic (IP₂₅ and II)
178 HBIs according to Eq. 2.

179 (2)

$$180 \quad \text{H - Print \%} = \frac{\text{(III)}}{(\text{IP}_{25} + \text{II} + \text{III})} \times 100$$

181 In addition to quantifying sympagic carbon contribution to amphipod diet using equation 1,
182 estimates of the proportion of sympagic carbon (with 99% confidence intervals), relative to
183 total marine carbon (i.e. sympagic plus pelagic), were also derived by converting H-Prints
184 using a previously modelled regression curve (Brown and Belt, 2017).

185

186 **Statistical analysis**

187 Statistical analysis was carried out in R-Studio version 1.0.136 (R-Core-Team, 2016).
188 ANOVA, with post-hoc Least Significant Difference mean separation tests (pairwise
189 comparisons), was used to compare iPOC_{amph} between amphipod species. A student’s t-test
190 for two samples was used to compare iPOC_{amph} between different size groups of the same
191 species. All data are reported as mean \pm standard error unless stated otherwise with tests
192 considered significant at $\alpha = 0.05$.

193

194 **RESULTS**

195 **Ice algae aggregates**

196 Taxonomic analysis of floating ice algal aggregates (1–15 cm in diameter) sampled within
197 the meltwater layer during the ICE12 cruise showed an assemblage of densely packed
198 diatoms, with a dominance of the ice-associated pennate diatoms *Navicula pelagica*,
199 *Hantzschia weyprechtii*, *Entomoneis paludosa* and *Cylindrotheca closterium* (Assmy *et al.*,
200 2013). Our analysis of one of these ice algal aggregates, which was sampled alongside
201 amphipods, showed a total organic carbon (TOC) content (261 ± 5 mg g⁻¹; 26%) consistent
202 with previous data from diatom cultures (e.g. *Berkeleya rutilans* 30%; Brown *et al.*, 2014b)
203 and floating ice algal aggregates (27–31%; Brown *et al.*, 2014c). The IP₂₅ content was
204 1.14 ± 0.02 μ g g⁻¹, giving an iPOC/IP₂₅ ratio of $2.29 \pm 0.04 \times 10^5$; $n = 6$. The dominance of sea
205 ice diatom species within the aggregate was also reflected in the H-Print (<1%; $n = 5$).

206

207 **iPOC in amphipods**

208 The mean abundance of the individual species, derived from 24 separate sampling operations
209 (Table 1, Fig. 3), showed that *Apherusa glacialis* (mean 7.7 ind. m⁻²) and *Onisimus nanseni*

210 (0.1 ind. m⁻²) were the most and least abundant species, respectively. The largest species,
211 *Gammarus wilkitzkii*, was the second most abundant (0.7 ind. m⁻²), while *Eusirus holmi* and
212 *Onisimus glacialis* were comparable (0.3 ind. m⁻²).

213 Our iPOC_{amph} estimates show that *G. wilkitzkii* contained the most iPOC, with
214 between 96 and 2052 µg C ind⁻¹ for specimens ranging in length from 15–40 mm (Fig. 4a-b).
215 Such specimens contained significantly more iPOC_{amph} than any other species, including *E.*
216 *holmi*, despite being of similar size ($F = 15.8$, $df = 4$, $p = <0.001$; Table 1). In general, larger
217 individuals of *G. wilkitzkii* (>35 mm) had ca. 4 times more iPOC_{amph} than smaller specimens
218 (<20 mm) ($t = 2.8$, $df = 9.3$, $p = 0.02$). Normalisation of iPOC_{amph} estimates to account for
219 amphipod mass (dry) revealed that *O. glacialis* had the highest dry mass (DM) normalised
220 iPOC_{amph}, with more than twice as much iPOC_{amph} as any other species ($F = 13.6$, $df = 4$, $p =$
221 <0.001 ; Table 1). In contrast to absolute iPOC_{amph} estimates, the DM normalised iPOC_{amph}
222 content of *G. wilkitzkii* was similar to the much smaller *A. glacialis* ($F = 13.6$, $df = 4$, $p =$
223 <0.001). Finally, DM normalised data revealed that *E. holmi* and *O. nanseni* had similar
224 iPOC_{amph} content, both being significantly less than other species (Table 1), despite their
225 difference in size (28±1.5 mm and 14±4 mm respectively).

226 The quantity of iPOC_{amph} per unit area of sea ice at the time of sampling was
227 estimated by combining mean iPOC_{amph} values with mean amphipod abundance derived from
228 the 24 separate observations made during sampling. This showed that the amount of iPOC
229 being retained by amphipods was ca. 0.66 mg iPOC m⁻² (Table 1). The majority of iPOC_{amph}
230 was found within *G. wilkitzkii* (73%; 0.48 mg m⁻²), followed by *A. glacialis* (19%), with *O.*
231 *glacialis*, *E. holmi* and *O. nanseni* containing the least (all <5%; 0.03 mg m⁻²). When
232 compared to the carbon standing stock of ice algal aggregates (0.74 mg C m⁻²; from Assmy *et*
233 *al.* (2013)), iPOC_{amph} in the five amphipod species corresponded to approximately 89% of
234 available ice algal aggregate carbon.

235

236 **Source of amphipod POC**

237 The majority (95%) of amphipod H-Prints for all species ranged from 0.1 to 7.2% (Fig. 4g-h),
238 with only four individuals (all *A. glacialis*) having H-Prints >7.2% (12.0, 13.1, 40.1 and
239 62.2%). Using the regression model defined previously by Brown and Belt (2017), these H-
240 Print values were re-expressed to estimate % sympagic carbon consumed by amphipods. In
241 all cases, mean % sympagic consumption was estimated as >90% (Table 1).

242

243 **DISCUSSION**

244 **Organic carbon and IP₂₅ content of sea ice algal aggregate**

245 The iPOC/IP₂₅ ratio used in the current study ($2.29 \pm 0.04 \times 10^5$) is much higher than that
246 reported previously for sea ice POC from Resolute Bay in the Canadian Arctic (ca. 2.6×10^3 ;
247 Brown *et al.*, 2016) and we provide two explanations for this. Firstly, in contrast to the
248 Resolute Bay sea ice samples, there were high amounts of extracellular polymeric substances
249 (EPS) in the ICE12 sea ice algal aggregates from the Arctic Ocean (Assmy *et al.*, 2013),
250 consistent with a ‘stressed/old’ community (Søreide *et al.*, 2006), and supported further by
251 observations of a large number of empty diatom frustules (Assmy *et al.*, 2013). In addition,
252 the percentage of IP₂₅-producing species in the ICE12 algae was lower (<0.1%) compared to
253 Resolute Bay (0.3–3.6%; Brown *et al.*, 2014c). Since ICE12 aggregates were sampled from
254 within the water column, rather than directly from within sea ice, this reduction could
255 potentially be due to the *in-situ* incorporation of non-IP₂₅ producing phytoplanktic species,
256 although Assmy *et al.* (2013) showed that the aggregate composition was dominated by ice-
257 associated diatoms and this is supported here by very low H-Prints (<1%). Instead, although
258 *Haslea crucigeroides*, a known producer of IP₂₅ (Brown *et al.*, 2014c), could be identified in
259 the ICE12 aggregates (T. A. Brown, pers. obs.), it was not sufficiently abundant to be

260 included in previous taxonomical reports (Assmy *et al.*, 2013). Indeed, the IP₂₅-producing
261 species (*H. crucigeroides*, *H. spicula*, *H. kjellmanii* and *Pleurosigma stuxbergii* var
262 *rhomboides*) are typically <1% of sea ice diatom assemblages from north-east Svalbard and
263 west Greenland (von Quillfeldt, 2000), while the same species comprised >3% of the diatoms
264 present in the Resolute Bay aggregates (Brown *et al.*, 2014c and references therein). In any
265 case, regardless of the exact reasons for the differences in iPOC/IP₂₅, this study reinforces the
266 importance of measuring this ratio on a case-by-case basis, as recommended by Brown *et al.*
267 (2016). In contrast, adoption of a fixed value for iPOC/IP₂₅ will likely lead to anomalous
268 estimates of iPOC within suspended/sinking POC and food-web constituents, as discussed in
269 detail by Brown *et al.* (2016).

270

271 **Quantitative estimates of ice-derived organic carbon in amphipods**

272 IP₂₅ was present in each of the amphipod specimens analysed, enabling us to estimate
273 iPOC_{amph} in all cases. iPOC_{amph} estimates varied by three orders of magnitude, broadly
274 reflecting the range in amphipod size, with the smallest (*A. glacialis*) and largest (*G.*
275 *wilkitzkii*) containing the lowest and highest iPOC_{amph}, respectively. Dry mass-normalised
276 abundances showed the opposite trend, however, with smaller species (and smaller
277 individuals of species) having relatively higher iPOC_{amph}, which aligns with smaller animals
278 having to sustain higher weight-specific ingestion rates to offset their higher metabolic
279 activity (c.f. larger animals) (Werner, 1997). On the other hand, this size-dependant
280 difference in iPOC_{amph} may potentially reflect the variable dietary preference of amphipods,
281 especially as the smaller *A. glacialis* are more herbivorous than the larger and mainly
282 omnivorous/carnivorous *G. wilkitzkii* (Poltermann, 2001).

283 Next, by expressing the iPOC_{amph} values as a percentage of estimated amphipod
284 carbon content (ca. 40%; Werner, 1997; Yuichiro and Tsutomu, 2003; Kiørboe, 2013; Fig

285 5e–f), our data show that <13% of amphipod body carbon comprised carbon derived from sea
286 ice algal aggregates, in good agreement with data obtained from captive *G. wilkitzkii*, *O.*
287 *nanseni* and *A. glacialis*, which consumed between 0.1 and 16% of body carbon during
288 experiments carried out in fixed-volume vessels containing physical ice substrate (Werner,
289 1997).

290 We then combined iPOC_{amph} data with the TOC content of ICE12 aggregates to
291 obtain estimates of the total mass of ice algae consumed by amphipods. Our data indicate that
292 individual *G. wilkitzkii* had consumed between 0.5 and 5 mg of ice algal aggregate leading up
293 to their capture during our sampling campaign. Since our data represent *in-situ* values, it is
294 not possible to definitively report data as estimates of daily consumption rates that would
295 facilitate direct comparisons with other studies. However, comparison of our iPOC_{amph}
296 estimates to consumption rates reported previously for *Gammarus* spp. feeding on
297 macrophytes in the Baltic Sea (1–5 mg ind. d⁻¹; Orav-Kotta *et al.*, 2009) and captive *G.*
298 *wilkitzkii* (0.08–0.14 mg algae ind. d⁻¹; Werner, 1997), indicate that our estimates likely also
299 reflect grazing rates over approximately 24 h. Further direct comparisons of iPOC/IP₂₅
300 derived values between *in-situ* and captive zooplankters might improve such comparisons in
301 the future.

302 Finally, by combining iPOC_{amph} with amphipod abundance (i.e. number of individuals
303 per unit area) for each of the five species, we estimate that iPOC_{amph} accounted for ca. 89% of
304 the available ice algal aggregate carbon during the course of sampling, which agrees well
305 with previous estimates of 63% and 58–92% (Siferd *et al.*, 1997; Kohlbach *et al.*, 2016).
306 Similarly, our consistent amphipod H-Prints indicate that most amphipod species appeared to
307 be obtaining energy almost exclusively (>90%; Table 1) from ice algal aggregates. On the
308 other hand, based on a composite of field-measured abundances and laboratory-based grazing
309 studies, Werner (1997) estimated the daily grazing impacts of *A. glacialis*, *Onisimus* spp. and

310 *G. wilkitzkii* to be ca. 1.1 and 2.6% for the Laptev and Greenland Sea, respectively. One
311 explanation for these different outcomes might be associated with the high degree of
312 variability in amphipod abundance, which is strongly seasonally dependent in response to the
313 development of sea ice (Siferd *et al.*, 1997; Werner and Auel, 2005). Thus, it is possible that
314 our amphipod abundances (and therefore estimates of grazing impact) were influenced, to
315 some extent, by the sea ice conditions during the late melt season, when the sea ice was
316 becoming increasingly heterogeneous, with a growing number of melt ponds (Assmy *et al.*,
317 2013). At this time in the season, after much of the iPOC had likely already been exported
318 (e.g. Brown *et al.*, 2016), it is also possible that ice algae aggregates represented an important
319 and concentrated food source in an otherwise relatively oligotrophic period. In this case,
320 amphipod diet at the time of sampling would likely be dominated by ice algae, rather than
321 other sources, resulting in relatively high estimates of grazing impact.

322 A part of iPOC_{amph} could have been acquired from other carbon sources since, for
323 example, large *G. wilkitzkii* has an omnivorous diet, and consumes both zooplankton and ice
324 amphipods (Werner, 1997; Sørenseide *et al.*, 2006). The most likely candidates of zooplankton
325 prey is *Calanus glacialis*, which is known to utilize ice algal blooms to fuel early maturation
326 and reproduction (Sørenseide *et al.*, 2010). Qualitative assessment of herbivory/carnivory in
327 amphipods has been established based on faecal pellet colouration, where green-yellow and
328 orange-red pigments indicate herbivory and carnivory, respectively (Werner, 2000).
329 Accordingly, the observed orange colouration of *G. wilkitzkii* lipid extracts in this study
330 likely indicates that this species incorporated at least some of the estimated iPOC_{amph} through
331 carnivory, likely from *Calanus* sp., rather than direct herbivory. Despite this, we note that our
332 *G. wilkitzkii* iPOC_{amph} data remain comparable to other captive grazing experiments where
333 carnivory was absent (Fig. 4 d,f; Werner, 1997). Indeed, it is well established that IP₂₅ is
334 transferred across trophic levels, and is readily identified in Arctic consumers, from fish

335 (Brown and Belt, 2012b; Brown *et al.*, 2015) and seabirds (Megson *et al.*, 2014), right up to
336 marine mammals (Brown *et al.*, 2013, 2014a).

337

338 **iPOC_{amph} in *Eusirus holmi***

339 In contrast to the other amphipod species in this study, comparison of iPOC_{amph} data with
340 literature values was not possible for *E. holmi*, despite this species being pan-Arctic in
341 distribution (Tencati and Geiger, 1968; Siferd, 2015). The limited reporting of *E. holmi* likely
342 reflects its low abundance in the Arctic, rather than difficulties in identification, as it is easily
343 recognized based on its light orange eyes, orange markings on coxa and pleopods, and four
344 long antennae and long leg segments. *Eusirus holmi* accounted for ca. 3% of the amphipods
345 in our samples and was even lower (<1%) in a previous study from the same region
346 (Macnaughton *et al.*, 2007). Our iPOC_{amph} data therefore likely represent the only
347 documented estimates of iPOC consumption for this species. Notably, absolute iPOC_{amph}
348 estimates in *E. holmi* were most similar to those for the smaller *A. glacialis* and *O. nanseni*,
349 while normalised (dry body mass) values were also comparable to the much smaller *O.*
350 *nanseni*. Although the paucity of literature data prevents us from assessing our iPOC_{amph}
351 estimate for *E. holmi* further, we note that, in contrast to the other species investigated here, a
352 relatively low iPOC_{amph} content for this species might imply that it obtained the majority of
353 its organic carbon from sources other than sea ice algae. *Eusirus holmi* is frequently observed
354 by divers in the water column, typically with legs spread out to suspend itself while slowly
355 sinking. It occasionally propels itself upwards with its large telson and then repeats the slow
356 sinking. This likely represents the feeding behaviour of *E. holmi* in the water column, but it
357 can also be observed clinging to the underside of sea ice. However, the consistent H-Print
358 values indicated that ca. 100% (86-115%; 99% CI) of marine carbon in amphipods was of
359 sympagic origin (Table 1). While there are a number of potential reasons for the low

360 iPOC_{amph} estimates, including, for example, selectivity during grazing, further analysis of this
361 species will be necessary before firmer conclusions can be made. What is clear, however, is
362 that the low field abundances of *E. holmi* in other studies and low iPOC_{amph} content estimated
363 here indicate that this species is currently of minor importance with respect to channelling the
364 sympagic carbon component into the ecosystem, at least in comparison to other more
365 abundant species in this study, particularly, *G. wilkitzkii* and *A. glacialis*.

366

367 Having focused here on a somewhat localised setting, we anticipate that further application of
368 this technique to a wider range of Arctic ice fauna and zooplankters has the potential to
369 improve our knowledge and understanding of the role that ice algae play in supporting the
370 broader Arctic ecosystem. Concomitant with the long-term trend of decreasing sea ice extent
371 and thickness (Barber *et al.*, 2015), a similar decline in ice-amphipods, particularly *G.*
372 *wilkitzkii* has occurred, with associated reduction of high-energy food to upper trophic
373 consumers (Hop *et al.*, 2013). Reduction in sea ice extent in Antarctica has similarly been
374 identified as one of the causes of the recent decline in Antarctic krill populations in the
375 Southern Ocean (Flores *et al.*, 2012), with impacts on higher trophic level animals (Reiss *et*
376 *al.*, 2017). In both polar areas, increased ridging in thinner ice may partly compensate for loss
377 in sea ice extent by creating complex structures as enhanced habitat for sympagic fauna
378 (Gradinger *et al.*, 2010; Melbourne-Thomas *et al.*, 2016). The more pelagic *E. holmi* may
379 increase in abundance with changing ice conditions towards thinner first-year ice and more
380 frequent open water in the Arctic Ocean. Under such a scenario, *E. holmi* may potentially
381 represent an alternative energy source to that currently derived from ice algae (and associated
382 amphipods) and, therefore, an important target for future research efforts. In any case, the
383 data generated from this, and subsequent studies, will provide the necessary numerical input
384 required to assist models in predicting the potential impact of declining Arctic sea ice extent

385 on sea ice biota, and further evaluation of sea ice algae as an energy source for other Arctic
386 consumers.

387

388

389

390 CONCLUSION

391 Our data provide evidence to support our initial hypothesis that combining sea ice-derived
392 iPOC/IP₂₅ data with IP₂₅ concentration data obtained from amphipods can provide realistic
393 estimates of the amount of sympagic organic carbon within these primary consumers.

394 Accordingly, we present quantitative estimates of iPOC for ice-associated amphipods and the
395 first documented assessment of the sympagic carbon content of the understudied *E. holmi*.

396 Our findings are also supported by data obtained from the same samples using a combined
397 biomarker approach (H-Print). The data generated from this, and subsequent studies, will
398 provide numerical input required to assist models in predicting the potential impact of
399 declining Arctic sea ice extent on sea ice biota, and to further evaluate sea ice algae as an
400 energy source for other Arctic consumers.

401

402

403 ACKNOWLEDGEMENTS

404 We are indebted to the captain and crew of RV *Lance*. We are also grateful to A Tonkin
405 (University of Plymouth) for carrying out CHN analysis of algal aggregates. Taxonomic
406 analyses were based on a contract with Institute of Oceanology, Sopot, Poland, with expertise
407 administered by Slawomir Kwasniewski. We are also grateful to the Associate Editor and an
408 anonymous reviewer for their helpful comments.

409

410 FUNDING

411 This work was supported by the award of a Research Project Grant from the Leverhulme
412 Trust (UK). The ICE2012 cruise was funded and conducted as part of the Centre for Ice,
413 Climate and Ecosystems (ICE) at the Norwegian Polar Institute.

414

415

416 Table 1. Mean (\pm se) and relative (%) amphipod abundance, ice-derived particulate organic carbon (iPOC_{amph}) and H-Print estimates (99% CI)
 417 of sympagic carbon, as a percentage of sympagic and pelagic marine carbon consumed, based on the regression model of Brown and Belt
 418 (2017).

Species	Abundance			iPOC _{amph}						H-Print estimates (%) of sympagic carbon								
	<i>n</i>	ind. m ⁻²	% of all species	<i>n</i>	μ g C ind ⁻¹	% of all species	Significant difference ¹	mg C g ⁻¹ DM	% of all species	Significant difference ¹	iPOC % amphipod C	Significant difference ¹	mg C m ⁻²	% of all species	Mean (99% CI)	Max (99% CI)	Min (99% CI)	Significant difference ¹
<i>Apherusa glacialis</i>	367	7.7	85	15	16.3 \pm 2.4	2	a	9.8 \pm 1.9	21	a	2.5 \pm 0.5	a	0.13	19	92 (78-106)	100 (86-115)	37 (24-52)	a
<i>Eusirus holmi</i>	12	0.3	3	14	54.7 \pm 8.3	6	a	1.6 \pm 0.2	3	b	0.4 \pm 0.1	b	0.01	2	100 (86-115)	100 (86-115)	100 (86-115)	b
<i>Onismus nanseni</i>	6	0.1	1	13	68.5 \pm 18.9	7	a	5.1 \pm 1.1	11	ab	1.3 \pm 0.3	ab	0.01	1	100 (86-115)	100 (86-115)	99 (84-113)	b
<i>Onismus glacialis</i>	15	0.3	3	10	107.5 \pm 14.5	12	a	23.5 \pm 4.5	49	c	5.9 \pm 1.1	c	0.03	5	100 (86-115)	100 (86-115)	100 (86-115)	b
<i>Gammarus wilkitzkii</i>	34	0.7	8	34	673.6 \pm 94.5	73	b	7.8 \pm 1.3	16	a	2.0 \pm 0.3	a	0.48	73	99 (84-113)	100 (86-115)	93 (79-108)	b

Total	$\frac{4}{3}$	9.1 4*	$\frac{8}{6}$	920.6*	47.8*	0.6 6*
-------	---------------	-----------	---------------	--------	-------	-----------

419 * Calculated from mean values

420 ¹ Least Significant Difference mean separation tests (pairwise comparisons), $\alpha = 0.05$

421 REFERENCES

- 422 Arndt, C. E. and Swadling, K. M. (2006) Crustacea in Arctic and Antarctic Sea Ice:
423 Distribution, diet and life history strategies. *Adv. Mar. Biol.* **51**, 197-315.
- 424 Arrigo, K. R. (2014) Sea ice ecosystems. *Ann. Rev. Mar. Sci.*, **6**, 439-467.
- 425 Assmy, P., Ehn, J. K., Fernández-Méndez, M., Hop, H., Katlein, C., Sundfjord, A., Bluhm,
426 K., Daase, M., Engel, A., Fransson, A., Granskog, M. A., Hudson, S. R., Kristiansen,
427 S., Nicolaus, M., Peeken, I., Renner, A. H. H., Spreen, G., Tatarek, A. and Wiktor, J.
428 (2013) Floating ice-algal aggregates below melting Arctic sea ice. *PLoS ONE*, **8**,
429 e76599.
- 430 Barber, D. G., Hop, H., Mundy, C. J., Else, B., Dmitrenko, I. A., Tremblay, J.-E., Ehn, J. K.,
431 Assmy, P., Daase, M., Candlish, L. M. and Rysgaard, S. (2015) Selected physical,
432 biological and biogeochemical implications of a rapidly changing Arctic Marginal Ice
433 Zone. *Progr. Oceanogr.*, **139**, 122-150.
- 434 Belt, S. T., Brown, T. A., Navarro-Rodriguez, A., Cabedo-Sanz, P., Tonkin, A. and Ingle, R.
435 (2012) A reproducible method for the extraction, identification and quantification of
436 the Arctic sea ice proxy IP₂₅ from marine sediments. *Anal. Methods*, **4**, 705-713.
- 437 Belt, S. T., Massé, G., Rowland, S. J., Poulin, M., Michel, C. and Leblanc, B. (2007) A novel
438 chemical fossil of palaeo sea ice: IP₂₅. *Org. Geochem.*, **38**, 16-27.
- 439 Belt, S. T., Massé, G., Vare, L. L., Rowland, S. J., Poulin, M., Sicre, M.-A., Sampei, M. and
440 Fortier, L. (2008) Distinctive ¹³C isotopic signature distinguishes a novel sea ice
441 biomarker in Arctic sediments and sediment traps. *Mar. Chem.*, **112**, 158-167.
- 442 Belt, S. T. and Müller, J. (2013) The Arctic sea ice biomarker IP₂₅: a review of current
443 understanding, recommendations for future research and applications in palaeo sea ice
444 reconstructions. *Quat. Sci. Rev.*, **79**, 9-25.

- 445 Brown, T. A. (2011) *Production and preservation of the Arctic sea ice diatom biomarker*
446 *IP₂₅*. *PhD Thesis*. University of Plymouth.
- 447 Brown, T. A., Alexander, C., Yurkowski, D. J., Ferguson, S. and Belt, S. T. (2014a)
448 Identifying variable sea ice carbon contributions to the Arctic ecosystem: A case
449 study using highly branched isoprenoid lipid biomarkers in Cumberland Sound ringed
450 seals. *Limnol. Oceanogr.*, **59**, 1581-1589.
- 451 Brown, T. A. and Belt, S. T. (2012a) Closely linked sea ice–pelagic coupling in the
452 Amundsen Gulf revealed by the sea ice diatom biomarker IP₂₅. *J. Plankton Res.*, **34**,
453 647-654.
- 454 Brown, T. A. and Belt, S. T. (2012b) Identification of the sea ice diatom biomarker IP₂₅ in
455 Arctic benthic macrofauna: Direct evidence for a sea ice diatom diet in Arctic
456 heterotrophs. *Polar Biol.*, **35**, 131-137.
- 457 Brown, T. A. and Belt, S. T. (2017) Biomarker-based H-Print quantifies the composition of
458 mixed sympagic and pelagic algae consumed by *Artemia* sp. *J. Exp. Mar. Biol. Ecol.*,
459 **488**, 32-37.
- 460 Brown, T. A., Chrystal, E., Ferguson, S. H., Yurkowski, D. J., Watt, C., Hussey, N. and Belt
461 S. T. (2017) Coupled changes in the sea ice carbon contribution to diet and trophic
462 position of Cumberland Sound beluga whales identified by H-Print and $\delta^{15}\text{N}$ analysis.
463 *Limnol. Oceanogr.* (In press).
- 464 Brown, T. A., Belt, S. T. and Cabedo-Sanz, P. (2014b) Identification of a novel di-
465 unsaturated C₂₅ highly branched isoprenoid in the marine tube-dwelling diatom
466 *Berkeleya rutilans*. *Environ. Chem. Lett.*, **12**, 455-460.
- 467 Brown, T. A., Belt, S. T., Ferguson, S. H., Yurkowski, D. J., Davison, N. J., Barnett, J. E. F.
468 and Jepson, P. D. (2013) Identification of the sea ice diatom biomarker IP₂₅ and
469 related lipids in marine mammals: A potential method for investigating regional

- 470 variations in dietary sources within higher trophic level marine systems. *J. Exp. Mar.*
471 *Biol. Ecol.*, **441**, 99-104.
- 472 Brown, T. A., Belt, S. T., Gosselin, M., Levasseur, M., Poulin, M. and Mundy, C. J. (2016)
473 Quantitative estimates of sinking sea ice particulate organic carbon based on the
474 biomarker IP₂₅. *Mar. Ecol. Prog. Ser.*, **546**, 17-29.
- 475 Brown, T. A., Belt, S. T., Philippe, B., Mundy, C. J., Massé, G., Poulin, M. and Gosselin, M.
476 (2011) Temporal and vertical variations of lipid biomarkers during a bottom ice
477 diatom bloom in the Canadian Beaufort Sea: Further evidence for the use of the IP₂₅
478 biomarker as a proxy for spring Arctic sea ice. *Polar Biol.*, **34**, 1857-1868.
- 479 Brown, T. A., Belt, S. T., Tatarek, A. and Mundy, C. J. (2014c) Source identification of the
480 Arctic sea ice proxy IP₂₅. *Nat. Comms.*, **5**, 4197.
- 481 Brown, T. A., Hegseth, E. N. and Belt, S. T. (2015) A biomarker-based investigation of the
482 mid-winter ecosystem in Rijpfjorden, Svalbard. *Polar Biol.*, **38**, 37-50.
- 483 Brown, T. A., Yurkowski, D. J., Ferguson, S. H., Alexander, C. and Belt, S. T. (2014d) H-
484 Print: a new chemical fingerprinting approach for distinguishing primary production
485 sources in Arctic ecosystems. *Environ. Chem. Lett.*, **12**, 387-392.
- 486 Dalpadado, P., Hop, H., Rønning, J., Pavlov, V., Sperfeld, E., Buchholz, F., Rey A, Wold, A.
487 (2016) Distribution and abundance of euphausiids and pelagic amphipods in
488 Kongsfjorden, Isfjorden and Rijpfjorden (Svalbard) and changes in their relative
489 importance as key prey in a warming marine ecosystem. *Polar Biol.*, **39**, 1765-1784.
- 490 Dieckmann, G. S. and Hellmer, H. H. (2010) The importance of sea ice: An overview. In: D.
491 Thomas and S. Dieckmann (eds) *Sea ice (second edition)*. Blackwell Publishing,
492 Chichester, pp. 1-22.
- 493 Flores, H., Atkinson, A., Kawaguchi, S., Krafft, B. A., Milinevsky, G., Nicol, S., Reiss, C.,
494 Tarling, G. A., Werner, R., Rebolledo, E. B., Cirelli, V., Cuzin-Roudy, J., Fielding,

- 495 S., Groeneveld, J. J., Haraldsson, M., Lombana, A., Marschoff, E., Meyer, B.,
496 Pakhomov, E. A., Rombola, E., Schmidt, K., Siegel, V., Teschke, M., Tonkes, H.,
497 Toullec, J. Y., Trathan, P. N., Tremblay, N., Van De Putte, A. P., Van Franeker, J. A.
498 and Werner, T. (2012) Impact of climate change on Antarctic krill. *Mar. Ecol. Prog.
499 Ser.*, **458**, 1-19.
- 500 Gradinger, R., Bluhm, B. and Iken, K. (2010) Arctic sea-ice ridges--Safe heavens for sea-ice
501 fauna during periods of extreme ice melt? *Deep-Sea Res. II*, **57**, 86-95
- 502 Hop, H., Bluhm, B. A., Daase, M., Gradinger, R., Poulin, M. (2013) Arctic Sea Ice Biota.
503 Arctic Report Cards, NOAA. <<http://www.arctic.noaa.gov/reportcard>>.
- 504 Hop, H., Poltermann, M., Lønne, O. J., Falk-Petersen, S., Korsnes, R., Budgell, W. P. (2000)
505 Ice amphipod distribution relative to ice density and under-ice topography in the
506 northern Barents Sea. *Polar Biol.*, **23**, 367-367.
- 507 Jakobsson, M., Mayer, L., Coakley, B., Dowdeswell, J. A., Forbes, S., Fridman, B.,
508 Hodnesdal, H., Noormets, R., Pedersen, R., Rebesco, M., Schenke, H. W.,
509 Zarayskaya, Y., Accettella, D., Armstrong, A., Anderson, R. M., Bienhoff, P.,
510 Camerlenghi, A., Church, I., Edwards, M., Gardner, J. V., Hall, J. K., Hell, B.,
511 Hestvik, O., Kristoffersen, Y., Marcussen, C., Mohammad, R., Mosher, D., Nghiem,
512 S. V., Pedrosa, M. T., Travaglini, P. G. and Weatherall, P. (2012) The International
513 Bathymetric Chart of the Arctic Ocean (IBCAO) Version 3.0. *Geophys. Res. Lett.*, **39**,
514 L12609.
- 515 Kiørboe, T. (2013) Zooplankton body composition. *Limnol. Oceanogr.*, **58**, 1843-1850.
- 516 Kohlbach, D., Graeve, M., Lange, B., David, C., Peeken, I. and Flores, H. (2016) The
517 importance of ice algae-produced carbon in the central Arctic Ocean ecosystem: Food
518 web relationships revealed by lipid and stable isotope analyses *Limnol. Oceanogr.*,
519 **61**, 2027-2044..

- 520 Kraft, A., Bauerfeind, E. and Nöthig, E.-M. (2010) Amphipod abundance in sediment trap
521 samples at the long-term observatory HAUSGARTEN (Fram Strait, ~79°N/4°E).
522 Variability in species community patterns. *Mar. Biodivers.*, **41**, 353-364.
- 523 Leu, E., Mundy, C. J., Assmy, P., Campbell, K., Gabrielsen, T. M., Gosselin, M., Juul-
524 Pedersen, T. and Gradinger, R. (2015) Arctic spring awakening – Steering principles
525 behind the phenology of vernal ice algal blooms. *Progr. Oceanogr.*, **139**: 151-170
- 526 Lønne, O. J. (1988) A diver-operated electric suction sampler for sympagic (=under-ice)
527 invertebrates. *Polar Res.*, **6**, 135-136.
- 528 Lønne, O. J., Gabrielsen, G. W. (1992) Summer diet of seabirds feeding in sea-ice-covered
529 waters near Svalbard. *Polar Biol.*, **12**, 685-692.
- 530 Lønne, O. J. and Gulliksen, B. (1989) Size, age and diet of polar cod, *Boreogadus saida*
531 (Lepechin 1773), in ice covered waters. *Polar Biol.*, **9**, 187-191.
- 532 Macnaughton, M., Thormar, J. and Berge, J. (2007) Sympagic amphipods in the Arctic pack
533 ice: redescrptions of *Eusirus holmii* Hansen, 1887 and *Pleusymtes karstensi* Barnard,
534 1959. *Polar Biol.*, **30**, 1013-1025.
- 535 Megson, D., Brown, T. A., Johnson, G. W., O’Sullivan, G., Bicknell, A. W. J., Votier, S. C.,
536 Lohan, M. C., Comber, S., Kalin, R. and Worsfold, P. J. (2014) Identifying the
537 provenance of Leach’s storm petrels in the North Atlantic using polychlorinated
538 biphenyl signatures derived from comprehensive two-dimensional gas
539 chromatography with time-of-flight mass spectrometry. *Chemosphere*, **114**, 195-202.
- 540 Melbourne-Thomas, J., Corney, S. P., Trebilco, R., Meiners, K. M., Stevens, R. P.,
541 Kawaguchi, S., Sumner, M. D. and Constable, A. J. (2016) Under ice habitats for
542 Antarctic krill larvae: Could less mean more under climate warming? *Geophys. Res.*
543 *Lett.*, **43**, 10322-10327.

- 544 Nygård, H., Vihtakari, M. and Berge, J. (2009) Life history of *Onisimus caricus* (Amphipoda:
545 Lysianassoidea) in a high Arctic fjord. *Aquat. Biol.*, **5**, 63-74.
- 546 Orav-Kotta, H., Kotta, J., Herkül, K., Kotta, I. and Paalme, T. (2009) Seasonal variability in
547 the grazing potential of the invasive amphipod *Gammarus tigrinus* and the native
548 amphipod *Gammarus salinus* (Amphipoda: Crustacea) in the northern Baltic Sea.
549 *Biol. Invasions*, **11**, 597-608.
- 550 Poltermann, M. (2001) Arctic sea ice as feeding ground for amphipods – food sources and
551 strategies. *Polar Biol.*, **24**, 89-96.
- 552 R-Core-Team (2016) R: A language and environment for statistical computing. *R Foundation*
553 *for Statistical Computing, Vienna, Austria*. pp. URL <http://www.R-project.org/>.
- 554 Reiss, C. S., Cossio, A., Santora, J. A., Dietrich, K. S., Murray, A., Mitchell, B. G., Walsh, J.,
555 Weiss, E. L., Gimpel, C., Jones, C. D. and Watters, G. M. (2017) Overwinter habitat
556 selection by Antarctic krill under varying sea-ice conditions: implications for top
557 predators and fishery management. *Mar. Ecol. Prog. Ser.*, **568**, 1-16.
- 558 Serreze, M. C., Crawford, A. D., Stroeve, J. C., Barrett, A. P. and Woodgate, R. A. (2016)
559 Variability, trends, and predictability of seasonal sea ice retreat and advance in the
560 Chukchi Sea. *J. Geophys. Res. Ocean.*, **121**, 7308-7325.
- 561 Siferd, T. D. (2015) Central and Arctic Multi-Species Stock Assessment Surveys Version 5
562 In OBIS Canada Digital Collections. Bedford Institute of Oceanography, Dartmouth,
563 NS, Canada. Published by OBIS, Digital <http://www.iobis.org/>. Accessed on 15-12-
564 2016.
- 565 Siferd, T. D., Welch, H. E., Bergmann, M. A. and Curtis, M. F. (1997) Seasonal distribution
566 of sympagic amphipods near Chesterfield Inlet, N.W.T., Canada. *Polar Biol.*, **18**, 16-
567 22.

- 568 Søreide, J. E., Carroll, M. L., Hop, H., Ambrose Jr., W. G., Hegseth, E. N., and Falk-
569 Petersen, S. (2013) Sympagic-pelagic-benthic coupling in Arctic and Atlantic waters
570 around Svalbard revealed by stable isotopic and fatty acid tracers. *Mar. Biol. Res.*, **9**,
571 831-850.
- 572 Søreide, J. E., Hop, H., Carroll, M. L., Falk-Petersen, S. and Hegseth, E. N. (2006) Seasonal
573 food web structures and sympagic–pelagic coupling in the European Arctic revealed
574 by stable isotopes and a two-source food web model. *Progr. Oceanogr.*, **71**, 59-87.
- 575 Søreide, J. E., Leu, E., Berge, J., Graeve, M. and Falk-Petersen, S. (2010) Timing in
576 blooms, algal food quality and *Calanus glacialis* reproduction and growth in a
577 changing Arctic. *Glob. Change Biol.*, **16**, 3154-3163.
- 578 Tencati, J. R. and Geiger, S. R. (1968) Pelagic amphipods of the slope waters of Northeast
579 Greenland. *J. Fish. Res. Board Can.*, **25**, 1637-1650.
- 580 von Quillfeldt, C. H. (2000) Common diatom species in Arctic spring blooms: their
581 distribution and abundance. *Bot. Mar.*, **43**, 499-516.
- 582 Werner, I. (1997) Grazing of Arctic under-ice amphipods on sea-ice algae. *Mar. Ecol. Prog.*
583 *Ser.*, **160**, 93-99.
- 584 Werner, I. (2000) Faecal pellet production by Arctic under-ice amphipods – transfer of
585 organic matter through the ice/water interface. *Hydrobiologia*, **426**, 89-96.
- 586 Werner, I. and Auel, H. (2005) Seasonal variability in abundance, respiration and lipid
587 composition of Arctic under-ice amphipods. *Mar. Ecol. Prog. Ser.*, **292**, 251-262.
- 588 Yuichiro, Y. and Tsutomu, I. (2003) Metabolism and chemical composition of four pelagic
589 amphipods in the Oyashio region, western subarctic Pacific Ocean. *Mar. Ecol. Prog.*
590 *Ser.*, **253**, 233-241.

591

592

593 Figure captions

594

595 Fig. 1 Structures of sea ice diatom (IP₂₅, II) and phytoplanktic diatom (III) highly branched
596 isoprenoids (HBIs) measured in amphipods.

597

598 Fig. 2 Study location north of Svalbard with bathymetry. Green line is the drift trajectory of
599 the ice floe that the RV *Lance* was moored to, with start and end dates. The ice edge positions
600 for 27, 31 July and 2 August are indicated by the broken lines and are representative for the
601 drift period. Map created by the Norwegian Polar Institute, Max König. Bathymetry with
602 permission from IBACO (Jakobsson *et al.*, 2012).

603

604 Fig. 3 Averaged amphipod abundance for each species beneath the ice floe during sampling
605 (note: logged y-axis). Circles = flat under-ice surface, squares = ridged under-ice surface.

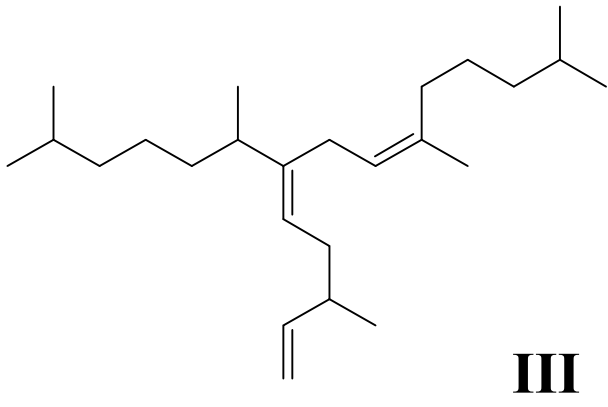
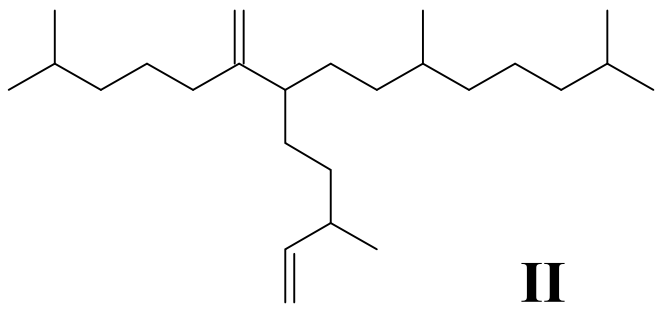
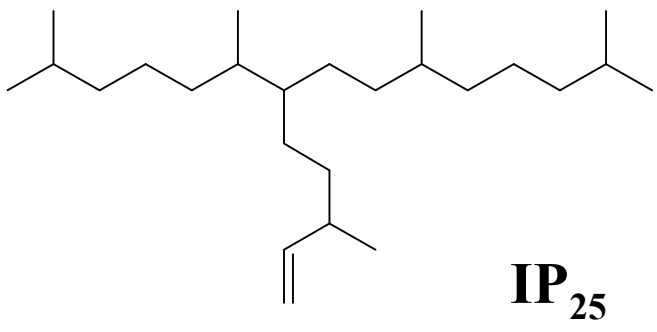
606

607 Fig. 4 Amphipod iPOC content (a-f) and H-Print (g-h; note logged scale) compared to
608 amphipod length (left) and for species average (right). Horizontal dotted lines (a, b) represent
609 equivalent total algal aggregate mass consumed for selected iPOC concentrations (note
610 logged scale in b). Red dots (d and f) show data derived from laboratory experiments
611 (Werner, 1997). Green dots (h) show the H-Print value derived from ice algal aggregates that
612 amphipods were observed grazing upon in this study.

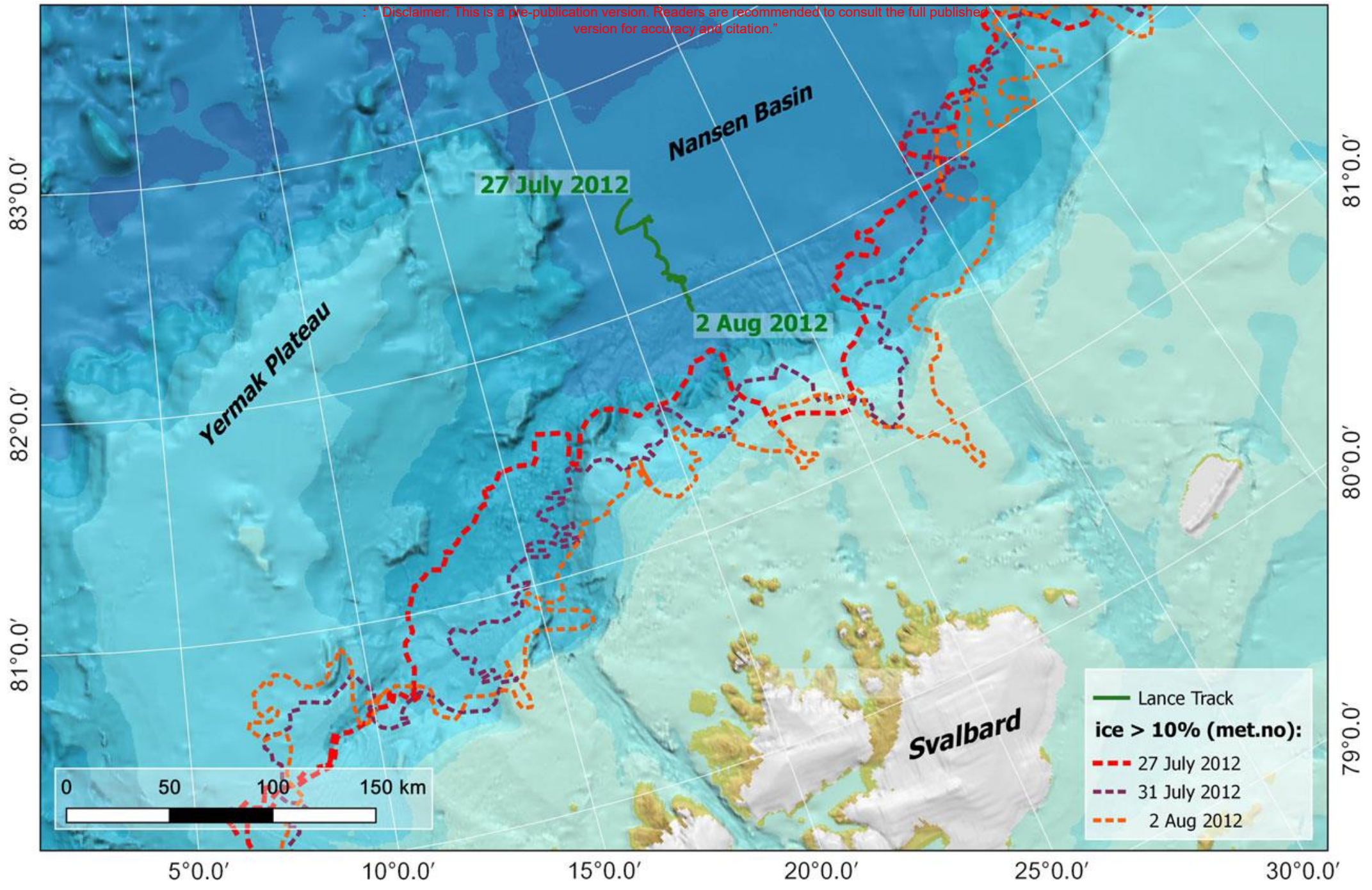
613

614

615



: "Disclaimer: This is a pre-publication version. Readers are recommended to consult the full published version for accuracy and citation."



: "Disclaimer: This is a pre-publication version. Readers are recommended to consult the full published version for accuracy and citation."

